

Accepted Manuscript (Post-print)

Title: Energy efficiency hexapod walking robot for humanitarian demining
Authors: Hector Montes, Lisbeth Mena, Roemi Fernández, Manuel Armada
Accepted for publication in: Industrial Robot: An International Journal
Publisher: Emerald Publishing

This is the author's accepted manuscript (AAM).

Final published version: <https://doi.org/10.1108/IR-11-2016-0281>

© 2017 Authors. For non-commercial use per publisher policy.



ENERGY EFFICIENCY HEXAPOD WALKING ROBOT FOR HUMANITARIAN DEMINING

Journal:	<i>Industrial Robot</i>
Manuscript ID	IR-11-2016-0281
Manuscript Type:	Original Manuscript
Keywords:	Hexapod walking robot, Energy efficiency, Humanitarian demining, Scanning manipulator, Power consumption

SCHOLARONE™
Manuscripts

Industrial Robot

ENERGY EFFICIENCY HEXAPOD WALKING ROBOT FOR HUMANITARIAN DEMINING

Abstract

Purpose – the aim of this paper is to introduce a hexapod walking robot specifically designed for applications in humanitarian demining, intended to operate autonomously for several hours. To this end the paper presents an experimental study for the evaluation of its energy efficiency.

Design/methodology/approach – first, the interest of using a walking robot for detection and localization of anti-personnel landmines is described, followed by the description of the mechanical system and the control architecture of the hexapod robot. Secondly, the energy efficiency of the hexapod robot is assessed in order to demonstrate its autonomy for performing humanitarian demining tasks. To achieve this, the power consumed by the robot is measured and logged, with a number of different payloads placed on board (including always the scanning manipulator arm assembled on the robot front end), during the execution of a discontinuous gait on flat terrain.

Findings – the hexapod walking robot has demonstrated low energy consumption when it is carrying out several locomotion cycles with different loads on it, which is fundamental in order to have a desired autonomy. It should be considered that the robot has a mass of about 250 kg, and that it has been loaded with additional masses of up to 170 kg during the experiments, with a consumption of mean power of 72 W, approximately.

Originality/value – This work provide insight on the use of a walking robot for humanitarian demining tasks, which has high stability and an autonomy of about three hours for a robot with high mass and high payload. In addition, the robot can be supervised and controlled remotely, which is an added value when it is working in the field.

Keywords Hexapod walking robot, energy efficiency, humanitarian demining, scanning manipulator

Paper type Research paper

1. Introduction

Detection and removal of landmines from the infested fields is a severe problem with vast political, social and economic dimensions, which have been present during the last decades (Baudoin et al., 1999). In this context, the international scientific community has shown a broad interest to solve this problem, which has been addressed from different points of view and with different procedures (Hirose and Kato, 1998; Nonami et al., 2003; Gonzalez de Santos, et al., 2007; Fukushima et al., 2008; Baudoin and Doroftei, 2012; Fernández et al., 2012; Montes et al., 2015b; Fernández et al., 2016; Montes et al., 2016). The anti-personnel mines, sub-munitions and unexploded ordnance (UXO) could remain active for several years (in some cases up to fifty years), they do not discriminate between military and civilian people, killing or injuring indiscriminately to them, including children and humanitarian collaborators (ICBL, 2010).

Currently, no one knows just how many buried landmines are in the world, but the number is in tens of millions (ICBL, 2014). However, some countries keep stockpiles that collectively

2

totalise around 50 million landmines. These countries (35) are outside the Mine Ban Treaty (ICBL, 2015). Regarding the buried landmines, one solution to this problem could be the application of fully automatic systems or tele-operated systems to detect and remove the landmines. However, regardless of the latest advances in this field, this solution seems to be not very close to being carried out.

In order to solve this humanitarian problem, using the above mentioned systems, it should be considered efficient sensors, detectors and positioning systems for detecting, locating and identifying the landmines. Besides, appropriate mobile vehicles should be developed in order to have on board the appropriated sensors for moving them over the mine fields, and, in this way, relieving human operator from direct risk. Additionally, it should be interesting to achieve human-robot collaboration to carry out the humanitarian demining tasks, since this work is very complex and difficult to realize.

Many types of mobile vehicles that could take on board sensors to displace them over a mine-infested area, e.g., wheeled vehicles, tracked vehicles and even legged robots, have been proposed to perform demining tasks efficiently and safely. Wheeled robots are the simplest, least costly and easily to control (Kopacek and Silberbauer, 2008; Fukushima, 2008; Baudoin et al., 2011; Baudoin and Doroftei, 2012); tracked robots have excellent ability to travel on almost any terrain (Baudoin et al., 1999; Munsang et al., 2002; Waterman et al., 2005); legged robots have a very interesting potential for this activity, nevertheless their control system is more complex (Gonzalez de Santos and Jimenez, 1995; Habumuremyi, 1998; Hirose and Kato, 1998; Gonzalez de Santos et al., 2002; Nonami et al., 2003; Gonzalez de Santos et al, 2007).

Legged robots for undertaking humanitarian demining tasks have been developed, at least, in the last 15 years, and several prototypes of these robots have been tested experimentally. Some examples of these robotics platforms are TITAN VIII (Hirose and Kato, 1998), AMRU-2 (Habumuremyi, 1998), RIMHO2 (Gonzalez de Santos and Jimenez, 1995), COMET series (Nonami et al., 2003), SILO6 (Gonzalez de Santos et al., 2002; Gonzalez de Santos et al, 2007), AMRU5 (Doroftei and Baudoin, 2012). Most of these walking robots are based on leg configurations of insect or mammal type. But there have been developed other configurations of walking robots for demining, such as sliding frame systems (Habumuremyi, 1998; Marques et al, 2002). The need to develop legged robots to operate in certain situations where other humanitarian demining systems using wheels or tracks cannot operate properly or have low yield, have been investigated by several research centres (Royal Military Academy (RMA), Free University of Brussels, Chiba University, Tokyo Institute of Technology, The Spanish National Research Council (CSIC), and others).

On the other hand, some investigations have been realized in order to analyse the energy consumption in walking legged robots for several applications (Marhefka and Orin, 1997; Gonzalez de Santos et al., 2009; Sanz-Merodio et al., 2012). The main idea of these works is to minimize the energy consumption in legged robots by planning new gaits or by analysing different configurations of their legs, generally considering only their own weight. Mostly, in these works the theoretical analysis of energy consumption and simulation results were presented. Also, in two of them, some experimental results were described. These results were based for a specific robot (SILO6), considering only its mechanical characteristics. In this case, the legs were designed in RRR configuration in order to the robot executes gaits as an insect or mammal configuration. However, the results of these works only can be applied to the mentioned robot. In addition, this robot cannot bear high loads; therefore, if this were the case, the vibrations would be very noticeable.

In Zhu et al. (2014) is presented an optimal design of robot leg for reduce the energy consumption, which is a theoretical interesting work. But, the issues raised in this paper must be validated on a real walking robot. In other work the power consumption analysis is carried out on a hexapod robot using different central Pattern Generator Models (Grzelczyk at al., 2015). However, the leg configurations are not gravitationally decoupled and the robot cannot load big masses.

Another interesting work has been presented in Gonzalez-Rodriguez et al. (2014), where it is summarised a study of the advantages of use gravitationally decoupled actuations in legged robots, in order to obtain energy efficiency. The authors used the LEBREL robot to carry out the experimentation. However, it is not clear if the robot is able to bear relatively high payloads to carry out any application, e.g., to load a scanning manipulator to perform humanitarian demining tasks. Since, this manipulator could have a mass between 10-20 kg and installed on front of the robot, avoiding the undesired vibrations when it is scanning.

In this work the main characteristics of a hexapod robot, specifically designed to performing humanitarian demining tasks is presented. The main objective of this hexapod walking robot is to detect and localise antipersonnel mines by using an on-board scanning manipulator arm with a metal detector (or another suitable sensor) installed at the tool centre point of its end-effector. This robot uses the intrinsic advantages of the configuration of its legs, which are gravitationally decoupled. Besides, due to its compact structure design, it can bear high payloads with high stability in statically stable gaits. In addition, an experimental evaluation of the energy efficiency of the robot bearing several loads is carried out in order to assess its energy consumption. This paper is organised as follows. Section 2 describes the mechanical design and system architecture of the hexapod robot. Section 3 presents some experimental results when the robot executes an alternating tripod gait on flat surface within a controlled environment. Afterwards, Section 4 shows the results of the assessment of energy efficiency of the walking robot. Finally, some conclusions are offered in Section 5.

2. General configuration of the hexapod robot

The hexapod walking robot has been configured for carrying out humanitarian demining tasks according to the requirements investigated in TIRAMISU Project (<http://www.fp7-tiramisu.eu>). This legged robot will carry on-board a scanning manipulator of 5 DoF, several sensors to help the scanning tasks, one industrial computer, electronics, control/power cards, Wi-Fi wireless communication system, DGPS, batteries, and other devices and accessories. All of this represents its basic payload, which is far from its allowed full payload, because the robot's electromechanical configuration can bear a high payload up to 300 kg. This high load capability is intended to provide a stiff well-founded basis for the on-board manipulator, computers and other instruments, even during robot displacement. This will help to drastically reduce the undesired vibrations, which could affect the sensors measurements. This can happen in case of other legged robots with lower weight or other leg configuration (if they are compared with the hexapod robot described in this paper), that are prone to vibrations in their structure when interacting with the environment (especially when they are moving on uneven terrain). In that case such undesired vibrations could be transmitted to the scanning manipulator, limiting its performance or, simply, its functionality.

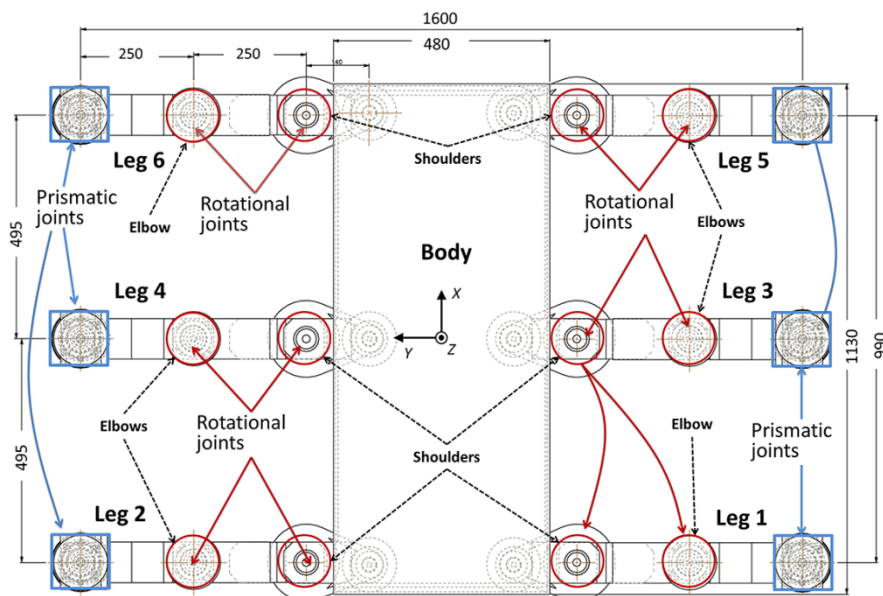
Some proposals of walking robot for humanitarian demining have been carried out in the last years and some references were cited in Section 1. For example, the SILO6 hexapod walking robot was developed for applications in humanitarian demining tasks (Gonzalez de Santos et al., 2002; Gonzalez de Santos et al, 2007; Sanz-Merodio, et al., 2012). This robot

4

use a mine detector installed on a scanning manipulator attached on front of its body. Encouraging results were obtained. However, the relationship of the manipulator mass with respect the robot mass was relatively high, and consequently a lot of vibrations were detected during the search of surrogate landmines in exploration tasks. Another example is the AMRU walking robot designed for humanitarian demining (Doroftei and Baudoin, 2012). Nevertheless, in the referenced paper, only some preliminary aspects concerning the robot design, its kinematics and control architecture are presented. Both robots have a different configuration and structure regarding to the robot presented in this article.

2.1. Description of the mechanical system

The hexapod robot legs have been designed following a SCARA configuration (RRP). This configuration presents the advantage to decouple gravitationally the vertical movement of the robot body from its horizontal movement, and so, the advancement of the robot can be achieved by the legs movements in the horizontal plane, which is not significantly affected by gravity (this applies obviously when the robot is walking on horizontal or with small slope surfaces; when there is some terrain inclination this decoupling advantage decreases, but in practice it still remains an interesting option). For this reason, with this leg design, this hexapod robot should have, at least in principle, an energetic autonomy relatively high, than with other possible configurations, what will be important considering its mass (~250 kg) and the payload that it can bear (<300 kg). Therefore, the scanning manipulator arm with metal detector and other sensors and devices installed on-board of this hexapod robot shall not implicate a significant load for it. Figure 1 shows the mechanical configuration of the hexapod robot. Table 1 shows the main characteristics of this walking inspection platform.



(a)

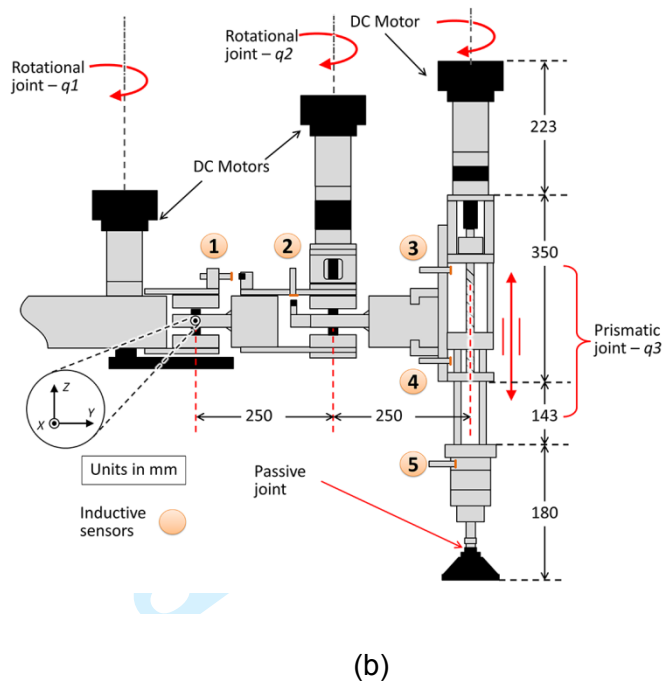


Figure 1. Mechanical configuration of the hexapod robot (units in mm). (a) Top view of the robot. (b) Frontal view of the leg.

Table 1. Main mechanical characteristics of the hexapod walking robot.

Degrees of freedom		18
Stability		High
Robot mass		254 kg
Payload capacity		Up to 300 kg
Obstacle height to surpass		Up to 200 mm
Power supply		16-30 VDC, Typ. 24 VDC
Body size	Length	1130 mm
	Width	480 mm
Robot size	Max length	1130 mm
	Max width	1700 mm

For the purposes of this paper, the main robot gait is performed by means of an alternating tripod gait mode. However, other gait alternatives have been developed in order to know the behaviour of the robot, being this out of the scope of this paper. With the alternating tripod gait, the hexapod has three feet in contact with the ground at all times, while the other legs are in transfer phase. In this gait two non-adjacent legs of one side and the central leg of the opposite side of the robot support the robotic platform, providing high stability, while the other tripod is in the transfer phase (Montes et al., 2015a; Montes et al., 2015b; Mena et al, 2016). The stability of this gait (in addition with the gravitational decoupling of the legs) is very important for carry out suitable humanitarian demining tasks using a detector installed on the scanning manipulator.

2.2. System architecture description

The system architecture of the hexapod robot consists of an on-board computer, control cards, data acquisition boards, power cards, signals conditioner cards, positioning sensors,

6

18 DC motors (three for each leg), Wi-Fi communication system, DGPS, batteries, and other devices and accessories used to control the scanning manipulator installed on front of the robot, i.e., a second computer on-board, mechanical devices, control and power cards, sensors, etc. This control architecture provides a reliable starting point for developing several control strategies in order to carry out humanitarian demining tasks. Figure 2 shows the most important subsystems that comprise the control architecture assembled in the hexapod robot, and a perspective view of the robot walking outdoors (Montes et al., 2015a; Montes et al., 2015b; Mena et al, 2016).

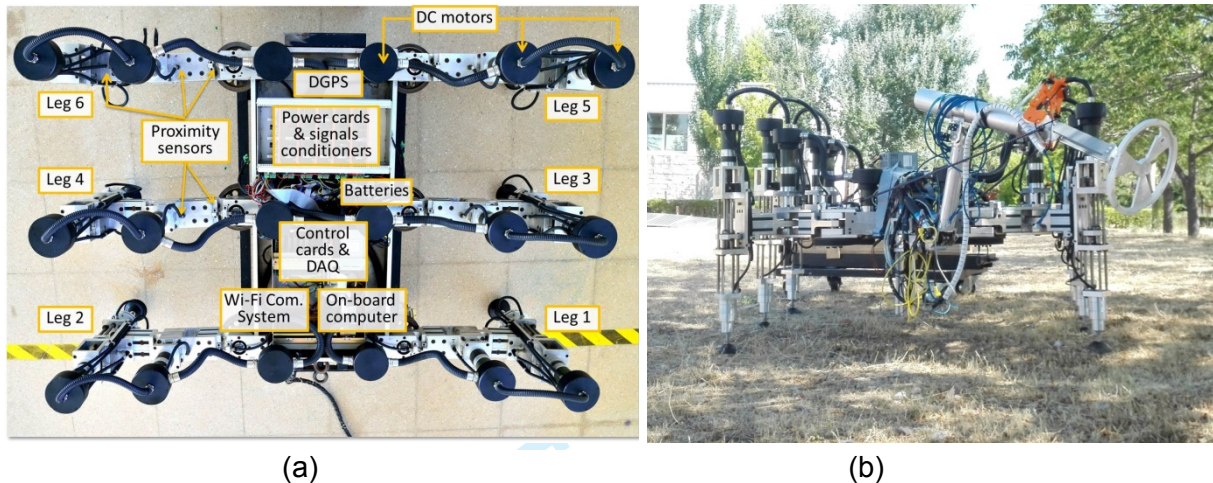


Figure 2. (a) Subsystems of the control architecture of the hexapod robot; (b) Hexapod walking robot at CSIC premises.

The central idea is to accomplish stable gaits in order that the scanning manipulator arm can perform suitable movements of its end-effector, where it is installed the metal detector head (or any other sensor like Ground Penetrating Radar). In this regard, the inspection platform shall move to a desired position so that the manipulator arm carries out the soil exploration. Standard strategies for the sweeping techniques will be considered, however the description of these strategies will not be considered in this paper, because the purpose of this manuscript is related only with the functioning of the hexapod robot. Nevertheless, some explanations related with these standards can be seen in (Fernández et al., 2012).

According to the strategies of demining tasks (supposing selected and commanded by an expert operator), the specific displacement of the robot is designated. These strategies are sent from control station to the main on-board computer in the robot, specifically, to the trajectory generator module by means of Wi-Fi communication. The trajectory generator uses the robot kinematics and the PID control system to execute the controlled movements of the hexapod robot. Figure 3 shows the general control architecture of the hexapod robot.

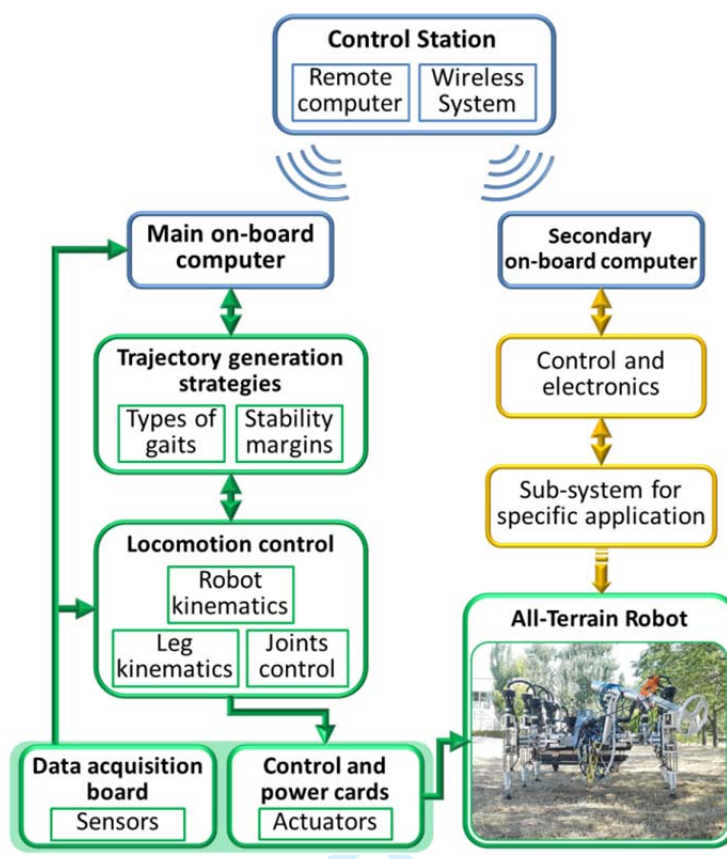


Figure 3. General control architecture of the hexapod robot.

3. Experimental results executing an alternating tripod gait

In order to obtain baseline data, several experimental tests with different gait patterns have been carried out at the CSIC lab. The hexapod robot has demonstrated high stability during the execution of several paths. During the firsts experiments, the robot moved loads of more than 50 kg (manipulator arm, second PC, other accessories and racks), and the additional power consumption has been insignificant with respect to the execution of gait patterns without extra payload. Therefore, it was demonstrated the feasibility to carry on-board of the robot the scanning manipulator and other additional sensors, where the additional masses does not contribute to significant extra energy consumption when the robot executes a trajectory. At the same time, the robot provides high stability in order to carry out special tasks, like looking for anti-personnel mines.

The algorithms for discontinuous and continuous gaits using the alternating tripod mode were implemented in the hexapod robot. Some experimental results about discontinuous gait are shown in Figure 4. In this case only the Cartesian positions of the extreme of the leg 1 (foot 1) of the robot are shown. The positions of the other leg feet have a similar behaviour, with analogous phase in the legs 1 and 5, but with 180° out-of-phase in the legs 2, 3 and 6. Only two steps are presented in Figure 4 in order to show some details of the experimental results. For this experiment, the reference coordinate frame is the shown in Figure 1(b), which it is in motion with the robot body. For this reason, the advance of the robot is not appreciated. The Y-axis drift of the leg 1 extreme position is appreciated in the second plot in Figure 4(a). However, this drift is about 1.0 mm in two steps, therefore, it can be corrected easily. This small drift is due to some backlashes that there are in the leg joints. In Figure

8

4(b) the transfer phase and stance phase of the leg 1 during two steps are shown. The damped small oscillations, observed in Y-axis, are related with the intrinsic forces produced by the contact of foot with the ground when the robot moves its body forward, in stance phase. However, these small oscillations can be negligible because are less than 0.5 mm.

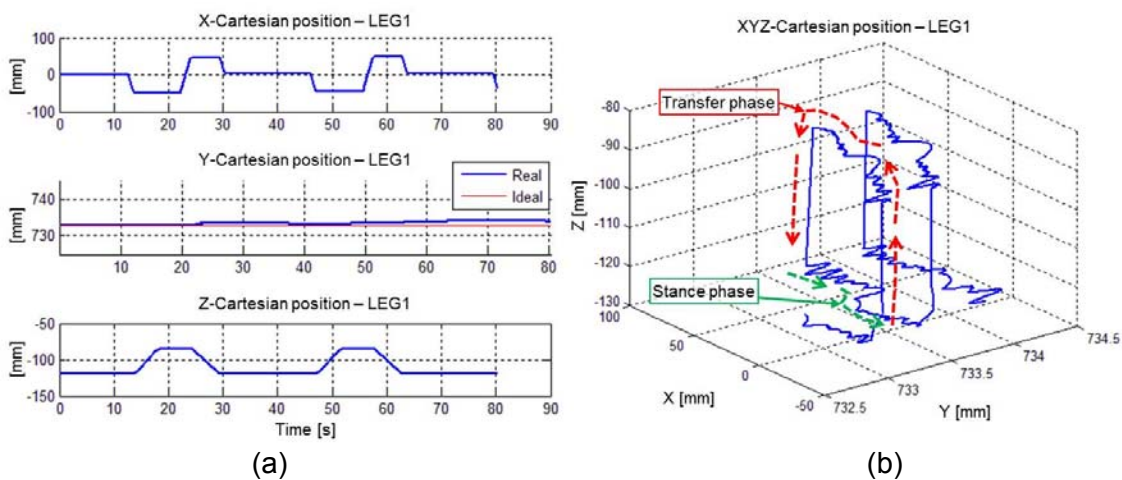


Figure 4. Some experimental results when performing an alternating tripod discontinuous gait. (a) Cartesian positions of the leg 1 extreme; (b) Phases of transfer and stance of leg 1.

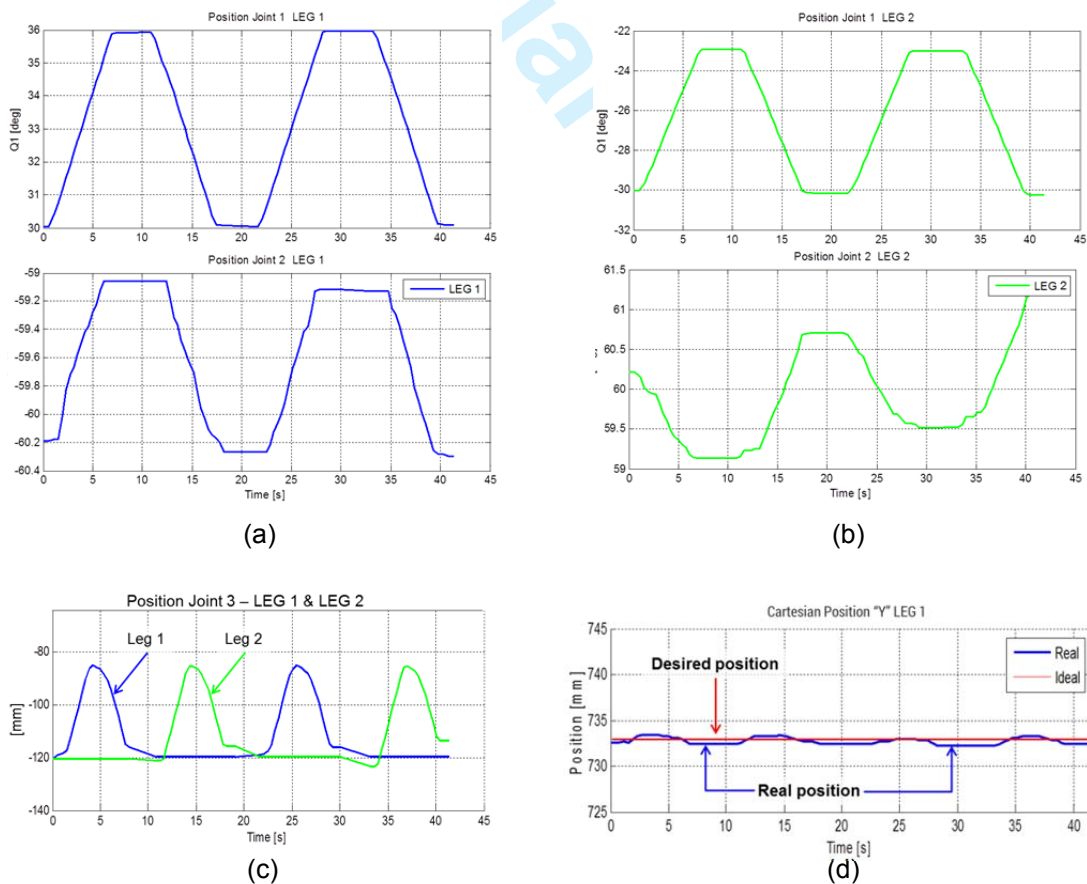


Figure 5. Some experimental results during the execution of a continuous gait using the alternating tripod mode.

Figure 5 shows some experimental results during the execution of a continuous gait using the alternating tripod mode. In order to notice some details of the experimental results, only two steps are presented in Figure 5. The coordinate reference is shown in Figure 1(b). Figures 5(a) and 5(b) show the angular position of the shoulder and elbow joints of the legs 1 and 2, respectively. Each of these legs moves within different tripods. For this reason, these graphics represent the motion of each tripod, assuming that the corresponding legs of each tripod have similar motions, which is right. In Figure 5(b), backlash in elbow joint of the leg 2 can be appreciated. This causes a small drift in the positioning of the leg-2 foot. Figure 5(c) shows the position of both legs ends along the Z axis. The alternating gait is perceived, besides a small unevenness on the soil is detected, between the interval $t=30s$ to $t=35s$. Figure 5(d) shows the lateral displacement of the leg 1 foot. The straight line of the trajectory commanded has an error about $\pm 0.51mm$, and it is considered reasonably low.

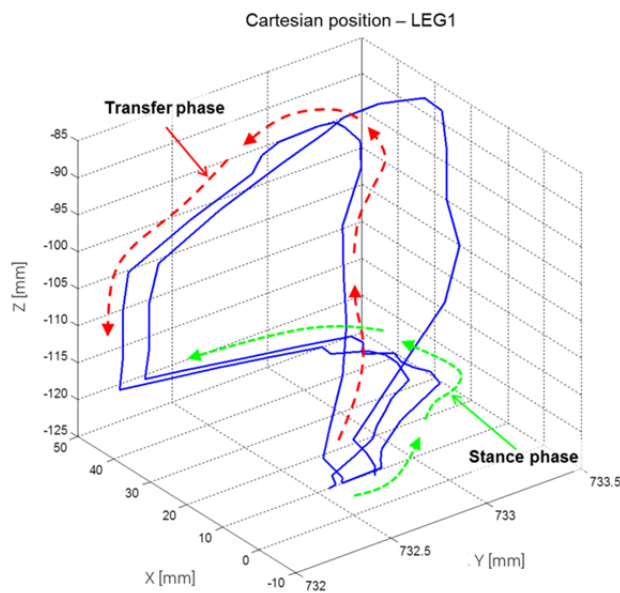


Figure 6. Phases of transfer and stance of the foot of leg 1 in a continuous gait.



Figure 7. Photographic sequence of a continuous gait pattern of the hexapod robot.

10

The transfer and stance phases of the foot of the leg 1 during two steps are shown in Figure 6. A small error along Y axis can be observed in this figure, besides of the small drift between each step. However, this drift is negligible for practical purposes. When the robot performs a gait during long time, e.g., when it is performing some humanitarian demining task (landmine searching), the summation of this error can be compensated by means of specific strategies in the control algorithm. Figure 7 shows a photographic sequence of a continuous gait pattern, with alternating tripod mode, of the hexapod robot at CSIC outdoor premises.

4. Assessment of the energy efficiency of the robot

As it was commented before, the legs of the hexapod walking robot have a SCARA configuration, and in this case the motion of the robot body is gravitationally decoupled (horizontal with respect to vertical), assuming the robot is moving close to horizontal surface (the robot can walk over uneven terrain with small slope, however this decoupling is evident). Consequently, the energy consumption is relatively low, even when the robot is subjected to bear high loads. This intrinsic functionality of the robot opens up the possibility to place on-board of the robot other sensors and instruments, as well as more powerful communication and computing devices.

In order to evaluate the energy efficiency of the hexapod robot, several experimental tests were carried out. First, as a starting point, let us consider that the robot has a mass of 250 kg. Second, in addition, the robot has on-board the scanning manipulator, the second on-board computer to control the manipulator, and other accessories. With this new load, the additional mass is about 65 kg, and then the system achieves the 315 kg, approximately. For initiating the experimentation phase a metal structure was installed on the robot, giving rise to a new mass of all-system of 320 kg, approximately. This makes the robot bears an initial payload of 70 kg, additional to its own structure. Then, some additional masses were added to the robot (step by step) up to achieve additional 100 kg. The power consumption was measured with each additional mass change while the robot carried out five steps in discontinuous gait with alternating tripod mode, as it was described in Section 3. Figure 8 shows some pictures with different loads on the hexapod robot during the experiments.

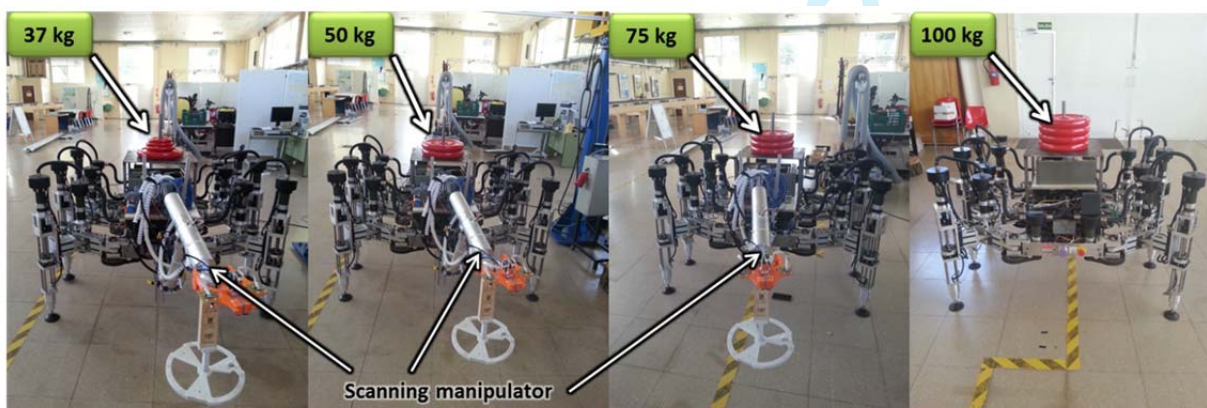


Figure 8. Photos with different loads put on the robot during the assessment of the energy consumption.

In order to calculate the power consumption during the trials with different masses on the robot, the instantaneous measurement of electric current and voltage of the electric actuators

installed in the robot were carried out. The main variable of the power consumption is the measured electric current, because it is continuously changing depending on the robot motion and the mass that it loads. On the other hand, the variation of the voltage is very small, and it can be considered constant, in this case, 24 VDC. However, in the calculation of the power consumption of the hexapod robot in the different trials, the measured instantaneous voltage has been considered, although its variation has been negligible. In Figure 9 two measurements of electric power consumption with additional masses of 0 kg and 100 kg are presented. The mean power consumption in the two trials is shown on the respective plot. Both masses (minimum and maximum) were selected in order to show the differences between the electric power signals during the experimentation. It could be noticed, that despite the big load change between both experiments (100 kg), the difference between the electric power consumption has not been very significant.

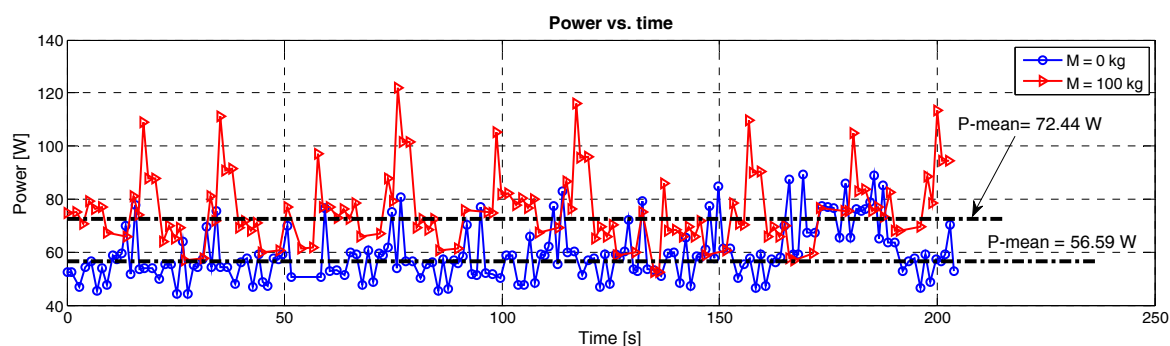


Figure 9. Electric power measurements in two trials: without extra mass, and with 100 kg of extra mass.

Figure 10 shows the results obtained from the experimental tests with several masses on the robot, while it carried out some steps in discontinuous gait (see Section 3). The electric power consumption was measured with the following masses (0, 12, 25, 37, 50, 62, 75, 100) kg, when the robot executed five steps on a flat surface. The relationship between the mean power consumption and the mass can be modelled by means of the next linear equation $P[\text{w}] = 0.1606M + 56.3815$. With this equation it is possible to extrapolate/interpolate the electric power consumption with masses greater than or less than 100 kg, respectively, in order to foresee what would be the energy that the robot would consume during the execution of a known trajectory (for this case, discontinuous gait with alternating tripod mode). In Figure 10 the mean power consumption of each trial is shown. As a relevant result from the experimental testing, with consumption of about 72 W of mean power, and no more of 120 W of maximum peak of power, this hexapod robot is able to move its own mass (250 kg), the scanning manipulator and its equipment and additional structure (70 kg), and 100 kg extra of mass, which represents a low consumption of energy. This is because to the intrinsic advantages of the configuration of robot legs, which decouple gravitationally the horizontal motion of this. Therefore, this system is energetically efficient when carries out displacements on quasi-horizontal soils.

12

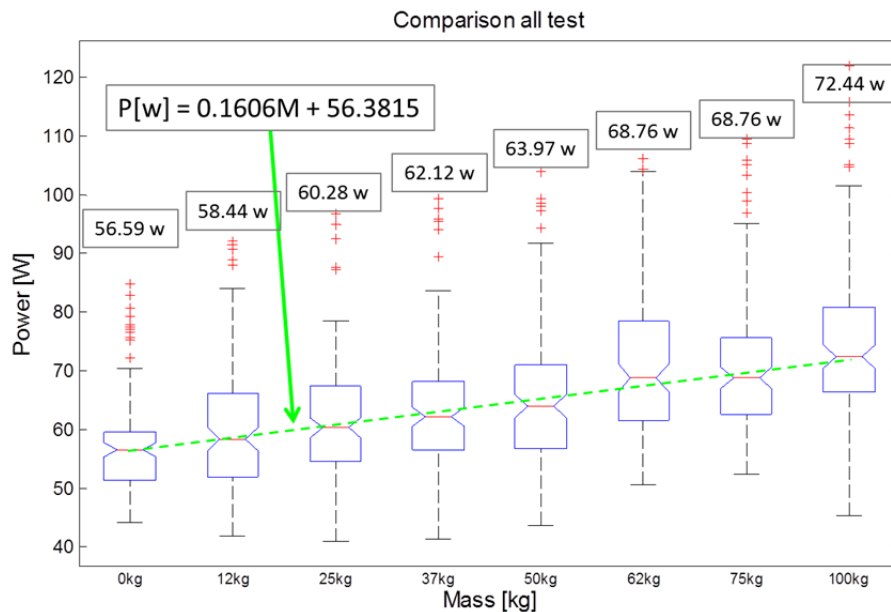


Figure 10. Results of the energy consumption of the robot gait with several loads on it.

This hexapod robot has a relatively high autonomy, which is based in two main reasons. The first is related to the low power consumption as has been stated above, due to the intrinsic advantages of the robot legs configuration; and secondly, due to the batteries capacity installed on board of the robot. Two batteries of 12 VDC, 20AH/20HR of lead-acid with Peukert's constant of 1.3, are connected in series in order to obtain 24 VDC to energize the servomotors.

The time of discharge the batteries is defined by Peukert's law, which expresses mathematically that as the rate of discharge increases, the available capacity of that battery decreases (see equation 1) (Hausmann and Depcik, 2013).

$$t = H \left(\frac{C}{IH} \right)^k \quad (1)$$

where,

t, is the time in hours of autonomy,

H, is the rated discharge time, in hours,

I, is the discharge electric current, in A,

C, is the rated capacity at that discharge rate, in A-h,

k, is the Peukert constant

Considering two cases established in the previous experimental results, i.e., when the robot did not carry on board any mass (total mass of 320 kg) and when it loaded 100 kg (total mass of 420 kg), the time of autonomy of the robot (discharge time of the battery) can be computed with equation 1. In both cases the electric current consumed by the on-board PC, the electronic boards, sensors, etc., was of 1.5 A, approximately. The mean electric currents for the first and second case were 2.36 A and 3.02 A, respectively. Consequently, the autonomy time of each of the cases was 3.45 h and 2.81 h, respectively.

On the other hand, the robot velocity range is dependent of the steps length and the gait strategies (Mena et al., 2016). In any case for this application the robot must walk at low

speeds in order to carry out the humanitarian demining tasks, because the searching of the landmines using a metal detector must be realized at a relatively low velocity, e.g., 0.1 to 0.3 m/s. For further details, see Fernandez et al. (2012). Normally, the lanes for localization of landmines have a width of 1.0 m, approximately (Fernandez et al., 2012). Therefore, with the extended manipulator to 0.6 m, with sensor head of 0.27 m of diameter, and carrying out scanning with overlap of half of the sensor head in each scanning, the robot is able to explore to a velocity 51.03 m²/h, approximately. Hence, it can be estimated the maximum coverage area for the two cases mentioned above, which are 176.05 m² for the first case and 143.39 m² for the second case. These results are very promising because in a short relative time the robot can cover a large area of infested landmine fields without compromising to the human operators. Besides, the robot can work without a break during the time of its autonomy, in contrast to human operators that must have breaks of 15 minutes every 45 minutes, at least (UNMAO, 2009).

5. Conclusions

In this paper a hexapod walking robot designed specifically for applications in humanitarian demining has been presented. This platform supports on-board a scanning manipulator arm, a second on-board computer and other accessories/equipment to detect and localize anti-personnel landmines. The first tests were carried out in indoor environment, and subsequent tests have been carried out in outdoor conditions; both tests within a controlled environments.

This hexapod robot with SCARA configuration legs can bear high payloads with low energy expenditure, which has been demonstrated with the experimental results described in this paper. In order to verify this statement, several tests were carried out. The power consumption of the hexapod robot was measured while it was executing several steps with different extra loads on it, as described in Section 4. The slope of the power consumption equation is very small (0.1606 W/kg), which validates the idea of the low consumption of energy using legs that decouple gravitationally the movement of the robot body. A mean power of 72 watts is low to move a mass of 420 kg, which consists of the robot system (320 kg) and the additional load of 100 kg. Besides having low energy consumption, the robot has demonstrated high stability to perform tasks that require some accuracy movements, such as those required for humanitarian demining tasks.

With the actual batteries, this robot has an autonomy of 2.81 h with an extra load of 100 kg, however, other set of batteries can be installed in order to increase twice as the autonomy of the actual system (the robot has capability of bear it). With this new autonomy the robot could perform landmine localization tasks similarly the human operators in 8 hours, without jeopardizing the physical integrity of human operators.

References

Baudoin, Y. and Doroffei, I. (2012), "TriDem - A Wheeled Mobile Robot for Humanitarian Mine Clearance". In Proc. 6th IARP Workshop on Humanitarian Demining (HUDEM), 24-26 April, Sibenik, Croatia, pp. 93-98.

Baudoin, Y., et al. (1999), Report: TASK 9, Humanitarian demining. Unpublished Manuscript. EC Brite/Euram TN on Climbing and Walking Robots, including the Support Technologies for Mobile Robotic Machines (CLAWAR), Year 2.

Baudoin, Y., Habib, M.K. and Doroftei, I. (2011). "Mobile robotics systems for humanitarian demining and risky interventions". In Baudoin, Y. and Habib, M.K. (Eds), Using robots in hazardous environments, Woodhead Publishing Ltd, Elsevier, UK, pp. 3-31.

Doroftei, I., and Baudoin, Y. (2012), A concept of walking robot for humanitarian demining. *Industrial Robot: An International Journal*, Vol. 39, Iss: 5, pp. 441-449.

Fernández, R., Montes, H., Salinas, C., González de Santos, P. and Armada, M. (2012), "Design of a training tool for improving the use of hand-held detectors in humanitarian demining". *Industrial Robot: An Intl. Journal*, Vol. 39, No. 5, pp. 450-463.

Fernández, R., Montes, H., Armada, M. (2016). Intelligent Multisensor Prodder for Training Operators in Humanitarian Demining. *Sensors*, Vol. 16, N° 7, p. 965.

Fukushima, E., Freese, M., Matsuzawa, T., Aibara, T. and Hirose, S. (2008), "Humanitarian demining robot gryphon. Current status and an objective evaluation". *Intl. Journal on Smart Sensing and Intelligent Systems*, Vol. 1, No. 3, pp.735-753.

Gonzalez de Santos, P. and Jimenez, M.A. (1995), "Generation of discontinuous gaits for quadruped walking machines". *Journal of Robotics Systems*, Vol. 12, No. 9, pp. 599-611.

Gonzalez de Santos, P., Cobano, J., Garcia, E., Estremera, J. and Armada, M. (2007), "A six-legged robot based system for humanitarian demining missions". *Mechatronics*, Vol. 17, pp. 417-430.

Gonzalez de Santos, P., Garcia, E., Estremera, J. and Armada, M.A. (2002), "Silo6: design and configuration of a legged robot for humanitarian demining". IARP Workshop on Robots for Humanitarian Demining, November 3-5, Vienna, Austria. Available at <http://www.gichd.org/fileadmin/pdf/LIMA/HUDEM2002.pdf> (accessed 14 June 2016).

Gonzalez de Santos, P., Garcia, E., Ponticelli, R. and Armada, M. (2009), "Minimizing energy consumption in hexapod robots". *Advanced Robotics*, Vol. 23, No. 6, pp. 681-704.

Gonzalez-Rodriguez, A. G., Gonzalez-Rodriguez, A., and Castillo-Garcia, F. (2014), Improving the energy efficiency and speed of walking robots. *Mechatronics*, Vol. 24, Iss. 5, pp. 476-488.

Grzelczyk, D., Stańczyk, B., and Awrejcewicz, J. (2015), Power consumption analysis of different hexapod robot gaits. In: *Proc. 13th International Conference Dynamical Systems - Theory and Applications*. December 7-10, Lodz, Poland, pp. 197-206.

Habumuremyi, J. C. (1998), "Rational designing of an electropneumatic robot for mine detection". In *First International Conference on Climbing and Walking Robots (CLAWAR'98)*, November, 26-28, Brussels, Belgium, pp. 267-273.

Hausmann, A., and Depcik, C. (2013), Expanding the Peukert equation for battery capacity modeling through inclusion of a temperature dependency. *Journal of Power Sources*, Vol. 235, pp. 148-158.

Hirose, S. and Kato, K. (1998), "Quadruped walking robot to perform mine detection and removal task". In *Proc. of the 1st International Conference on Climbing and Walking Robots*, Brussels, Belgium, pp. 261-266.

ICBL (2010), International campaign to ban landmines. 12th Annual Landmine Monitor report. Available at: http://www.the-monitor.org/media/1641811/Landmine_Monitor_2010_lowres.pdf (accessed 14 June 2016).

ICBL (2014), International campaign to ban landmines. Why Landmines are Still a Problem. Available at: <http://www.icbl.org/en-gb/problem/why-landmines-are-still-a-problem.aspx> (accessed 19 September 2016).

1
2
3
4
5
6
7 ICBL (2015), International campaign to ban landmines. 17th Annual Landmine Monitor
8 report. Available at: [http://www.the-monitor.org/media/2152583/Landmine-Monitor-](http://www.the-monitor.org/media/2152583/Landmine-Monitor-2015_finalpdf.pdf)
9 [2015_finalpdf.pdf](http://www.the-monitor.org/media/2152583/Landmine-Monitor-2015_finalpdf.pdf) (accessed 19 September 2016).

10 Kopacek, P. and Silberbauer, L. (2008), "A new Locomotion Concept for Humanitarian
11 Demining Robots". In 7th IARP International Workshop on Humanitarian Demining, El Cairo,
12 Egypt. March 28-30, pp. 32-36.

13
14 Marhefka, D.W. and Orin, D.E. (1997), "Gait planning for energy efficiency in walking
15 machines". IEEE Robotics and Automation Magazine, Vol. 97, pp. 474-478.

16
17 Marques, L., Rachkov, M. and Almeida, A.T. (2002), "Control system of a demining robot". In
18 Proc. of the 10th Mediterranean Conference on Control and Automation. Lisbon, Portugal.
19 Available at:
20 [https://www.researchgate.net/publication/236950634_Control_System_of_a_Demining_Robo](https://www.researchgate.net/publication/236950634_Control_System_of_a_Demining_Robot)
21 [t](https://www.researchgate.net/publication/236950634_Control_System_of_a_Demining_Robot) (accessed 14 June 2016).

22
23 Mena, L., Montes, H., Fernández, R., Sarria, J. and Armada, M. (2016). "Experimental
24 evaluation of the locomotion of a hexapod robot". In: Proc. RoboCity16 Open Conference on
25 Future Trends in Robotics, May 26-27, Universidad Politécnica de Madrid, Chapter 35, pp.
26 283-292. ISBN: 978-84-608-8452-1. Disponible en: [http://www.car.upm-csic.es/wp-](http://www.car.upm-csic.es/wp-content/uploads/2016/06/Proceedings_RoboCity16_web_version_01.pdf)
27 [content/uploads/2016/06/Proceedings_RoboCity16_web_version_01.pdf](http://www.car.upm-csic.es/wp-content/uploads/2016/06/Proceedings_RoboCity16_web_version_01.pdf)

28
29 Montes, H., Mena, L., Fernandez, R., Sarria, J. and Armada, M. (2015b), "Inspection platform
30 for applications in humanitarian demining". In Proc. 18th Intl. Conf. on Climbing and Walking
31 Robots and the Support Technologies for Mobile Machines. Sept. 6-9, HangZhou, China.
32 Assistive Robotics: pp. 446-453.

33
34 Montes, H., Mena, L., Fernández, R., Sarria, J., González de Santos, P. and Armada, M.
35 (2015a). "Hexapod robot for humanitarian demining". 8th IARP Workshop on Robotics for
36 Risky Environments (RISE 2015), Lisbon, Portugal. Available at:
37 [http://digital.csic.es/bitstream/10261/111656/1/Full_Paper_CSIC_8th_IARP_RISE2015_05.p](http://digital.csic.es/bitstream/10261/111656/1/Full_Paper_CSIC_8th_IARP_RISE2015_05.pdf)
38 [df](http://digital.csic.es/bitstream/10261/111656/1/Full_Paper_CSIC_8th_IARP_RISE2015_05.pdf) (accessed 14 June 2016).

39
40 Montes, H., Fernández, R., De Lorenzo, D., and Armada, M. (2016). Design and
41 implementation of a wireless prodder for instructional purposes in landmine detection.
42 Advances in Cooperative Robotics: pp. 348-355.

43
44 Munsang K., et al. (2002), "Development of a Mobile Robot with Double Tracks for
45 Hazardous Environment Applications (ROBHAZ-DT)". IARP Workshop on Robots for
46 Humanitarian Demining, November 3-5, Vienna, Austria. Available at
47 <http://www.gichd.org/fileadmin/pdf/LIMA/HUDEM2002.pdf> (accessed 14 June 2016).

48
49 Nonami, K., Huang, Q., Komizo, D. and Ikedo, Y. (2003), "Development and control of mine
50 detection robot comet-II and Comet-III". JSME International Journal, Series C, Vol. 46, N°3,
51 pp. 881-890.

52
53 Sanz-Merodio, D., Garcia, E. and Gonzalez de Santos, P. (2012), "Analyzing energy-efficient
54 configurations in hexapod robots for demining applications". Industrial Robot: An
55 International Journal, Vol. 39, No. 4, pp. 357-364.

56
57 UNMAO. (2009), Demining, not just a man's job. UNMAO news. The United Nations Mine
58 Action Office in Sudan. Available in: [http://reliefweb.int/sites/reliefweb.int/files/resources/](http://reliefweb.int/sites/reliefweb.int/files/resources/C446BBDF4C0CD8414925762300254482-Full_Report.pdf)
59 [C446BBDF4C0CD8414925762300254482-Full_Report.pdf](http://reliefweb.int/sites/reliefweb.int/files/resources/C446BBDF4C0CD8414925762300254482-Full_Report.pdf)

60
Waterman, D., Nonami, K., Yuasa, R., Amano, S., Masunaga, S. and Ono, H. (2005),
"Control and operational of a teleoperated hydraulic manipulator for landmine prodding and

1
2
3
4
5
6
7
8
9
10
11
12
13
14
15
16
17
18
19
20
21
22
23
24
25
26
27
28
29
30
31
32
33
34
35
36
37
38
39
40
41
42
43
44
45
46
47
48
49
50
51
52
53
54
55
56
57
58
59
60

16

excavation". In Proc. of the IARP International workshop on Robotics and Mechanical Assistance in Humanitarian Demining (HUDEM2005), Tokyo, June 2005, pp. 101-106.72.

Zhu, Y-G., Jin, B., Li, W, and Li, S-T. (2014), Optimal design of hexapod walking robot leg structure based on energy consumption and workspace. Transactions of the Canadian Society for Mechanical Engineering, Vol. 38, No. 3, pp. 305-317.

Industrial Robot

1
2
3
4
5
6
7
8
9
10
11
12
13
14
15
16
17
18
19
20
21
22
23
24
25
26
27
28
29
30
31
32
33
34
35
36
37
38
39
40
41
42
43
44
45
46
47
48
49
50
51
52
53
54
55
56
57
58
59
60

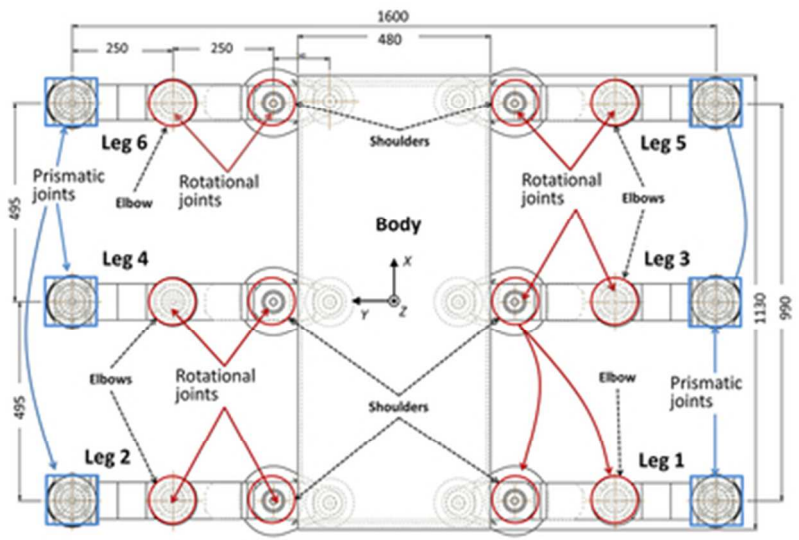


Figure 1. Mechanical configuration of the hexapod robot (units in mm). (a) Top view of the robot.

68x46mm (150 x 150 DPI)

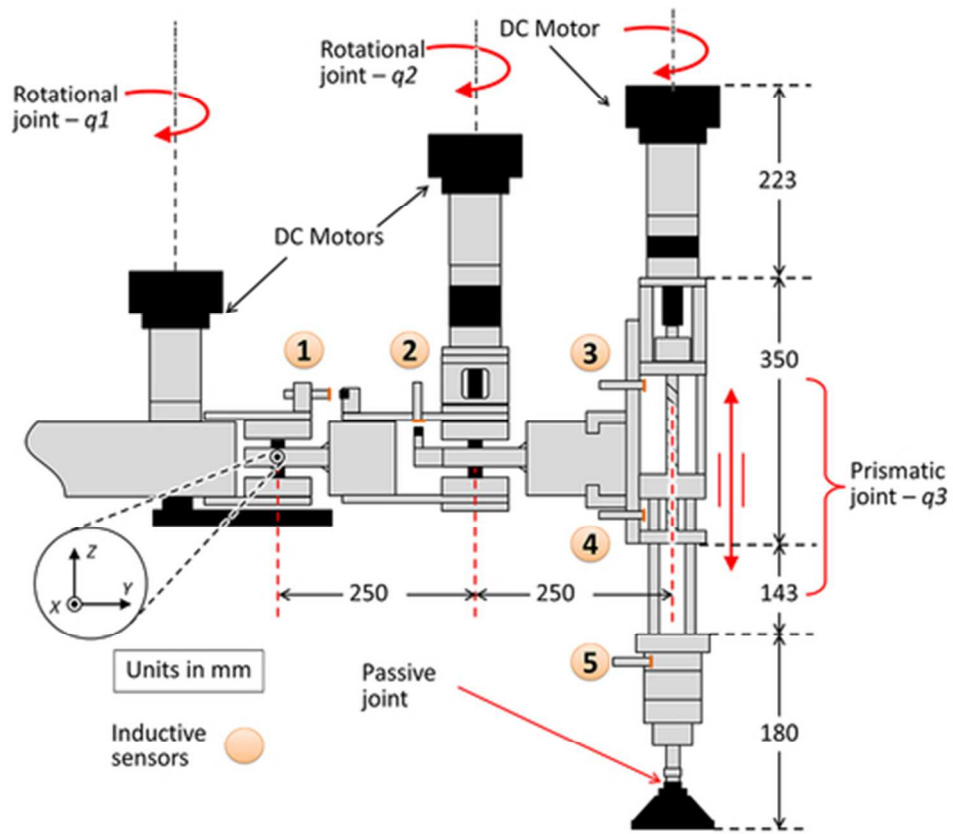


Figure 1. Mechanical configuration of the hexapod robot (units in mm). (b) Frontal view of the leg.

85x73mm (150 x 150 DPI)

dot

1
2
3
4
5
6
7
8
9
10
11
12
13
14
15
16
17
18
19
20
21
22
23
24
25
26
27
28
29
30
31
32
33
34
35
36
37
38
39
40
41
42
43
44
45
46
47
48
49
50
51
52
53
54
55
56
57
58
59
60

1
2
3
4
5
6
7
8
9
10
11
12
13
14
15
16
17
18
19
20
21
22
23
24
25
26
27
28
29
30
31
32
33
34
35
36
37
38
39
40
41
42
43
44
45
46
47
48
49
50
51
52
53
54
55
56
57
58
59
60



Figure 2. (a) Subsystems of the control architecture of the hexapod robot; (b) Hexapod walking robot at CSIC premises.

63x20mm (150 x 150 DPI)

Industrial Robot

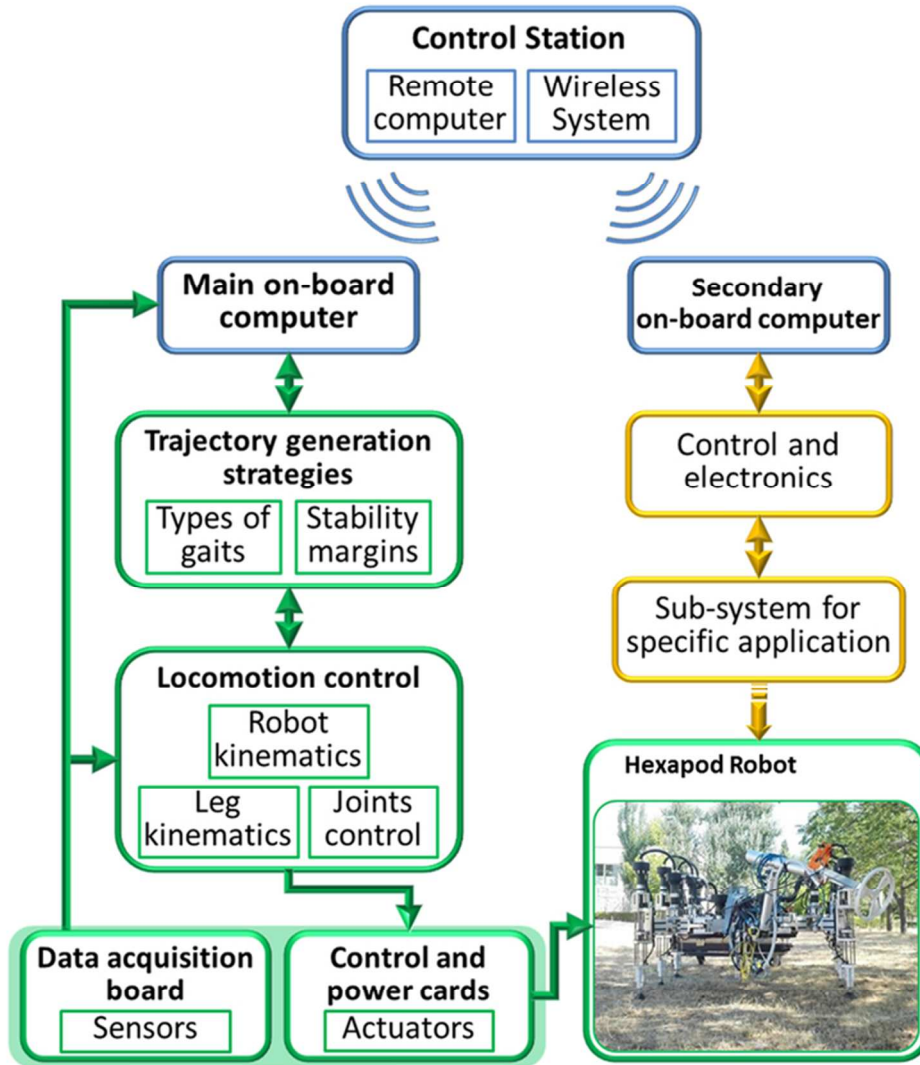


Figure 3. General control architecture of the hexapod robot.

132x146mm (150 x 150 DPI)

1
2
3
4
5
6
7
8
9
10
11
12
13
14
15
16
17
18
19
20
21
22
23
24
25
26
27
28
29
30
31
32
33
34
35
36
37
38
39
40
41
42
43
44
45
46
47
48
49
50
51
52
53
54
55
56
57
58
59
60

1
2
3
4
5
6
7
8
9
10
11
12
13
14
15
16
17
18
19
20
21
22
23
24
25
26
27
28
29
30
31
32
33
34
35
36
37
38
39
40
41
42
43
44
45
46
47
48
49
50
51
52
53
54
55
56
57
58
59
60

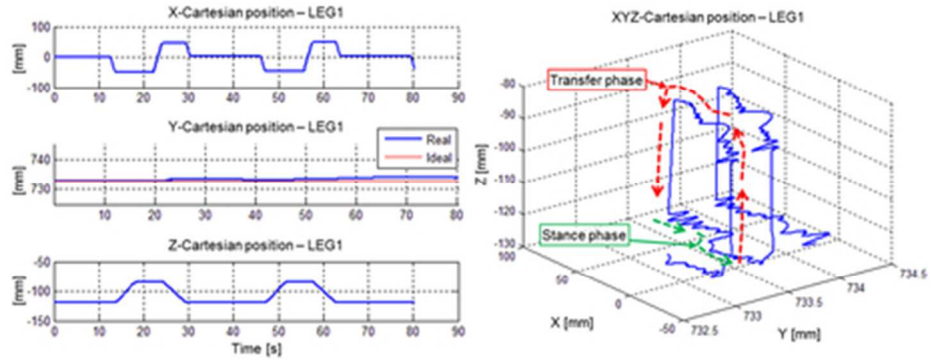


Figure 4. Some experimental results when performing an alternating tripod discontinuous gait. (a) Cartesian positions of the leg 1extreme; (b) Phases of transfer and stance of leg 1.

79x31mm (150 x 150 DPI)

Industrial Robot

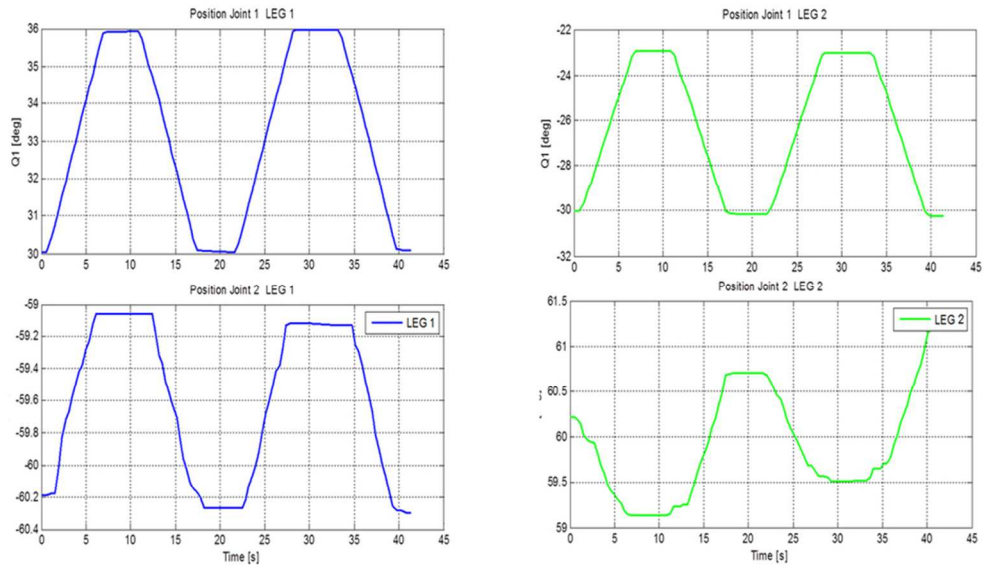


Figure 5. Some experimental results during the execution of a continuous gait using the alternating tripod mode.

160x96mm (150 x 150 DPI)

Industrial Robot

1
2
3
4
5
6
7
8
9
10
11
12
13
14
15
16
17
18
19
20
21
22
23
24
25
26
27
28
29
30
31
32
33
34
35
36
37
38
39
40
41
42
43
44
45
46
47
48
49
50
51
52
53
54
55
56
57
58
59
60

1
2
3
4
5
6
7
8
9
10
11
12
13
14
15
16
17
18
19
20
21
22
23
24
25
26
27
28
29
30
31
32
33
34
35
36
37
38
39
40
41
42
43
44
45
46
47
48
49
50
51
52
53
54
55
56
57
58
59
60

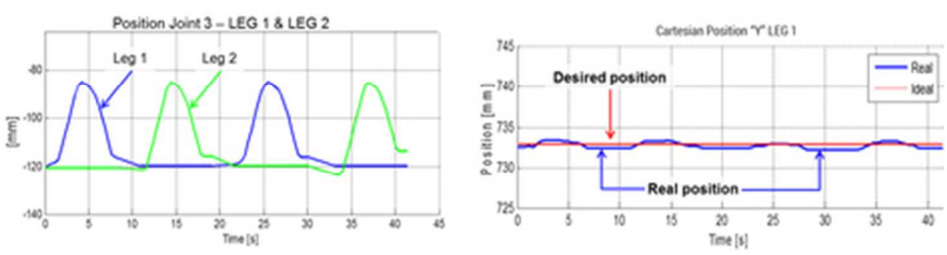
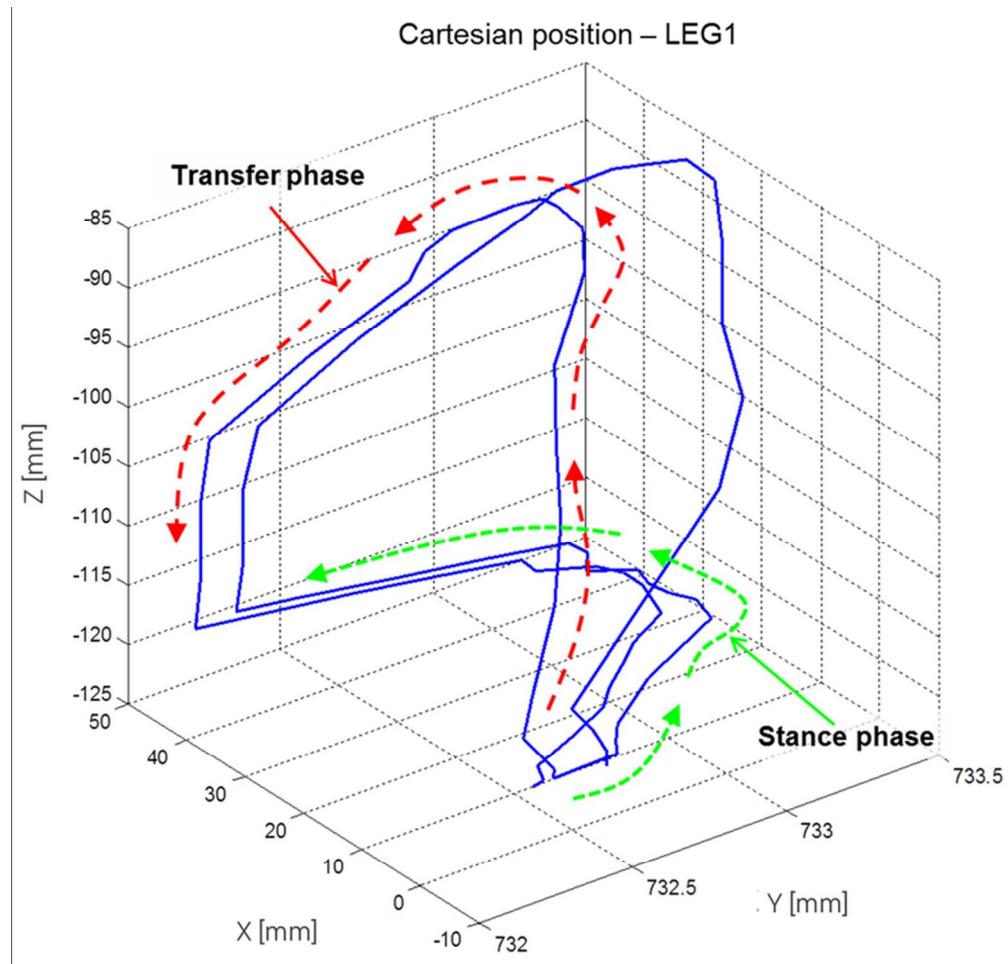


Figure 5. Some experimental results during the execution of a continuous gait using the alternating tripod mode.

81x22mm (150 x 150 DPI)

Industrial Robot



39 Figure 6. Phases of transfer and stance of the foot of leg 1 in a continuous gait.

40 144x138mm (150 x 150 DPI)



1
2
3
4
5
6
7
8
9
10
11
12
13
14
15
16
17
18
19
20
21
22
23
24
25
26
27
28
29
30
31
32
33
34
35
36
37
38
39
40
41
42
43
44
45
46
47
48
49
50
51
52
53
54
55
56
57
58
59
60



Figure 7. Photographic sequence of a continuous gait pattern of the hexapod robot.

75x28mm (150 x 150 DPI)

Industrial Robot

1
2
3
4
5
6
7
8
9
10
11
12
13
14
15
16
17
18
19
20
21
22
23
24
25
26
27
28
29
30
31
32
33
34
35
36
37
38
39
40
41
42
43
44
45
46
47
48
49
50
51
52
53
54
55
56
57
58
59
60



Figure 8. Photos with different loads put on the robot during the assessment of the energy consumption.

51x17mm (150 x 150 DPI)

Industrial Robot

1
2
3
4
5
6
7
8
9
10
11
12
13
14
15
16
17
18
19
20
21
22
23
24
25
26
27
28
29
30
31
32
33
34
35
36
37
38
39
40
41
42
43
44
45
46
47
48
49
50
51
52
53
54
55
56
57
58
59
60

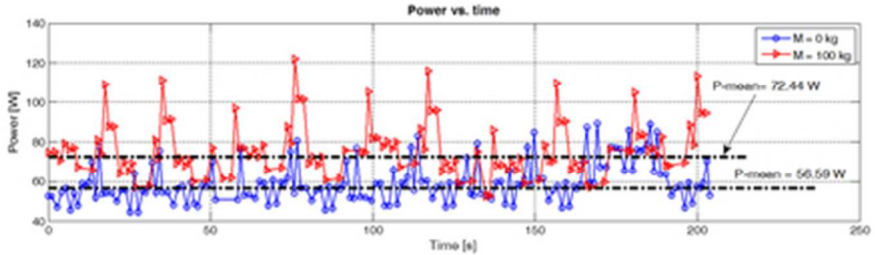


Figure 9. Electric power measurements in two trials: without extra mass, and with 100 kg of extra mass.

74x22mm (150 x 150 DPI)

Industrial Robot

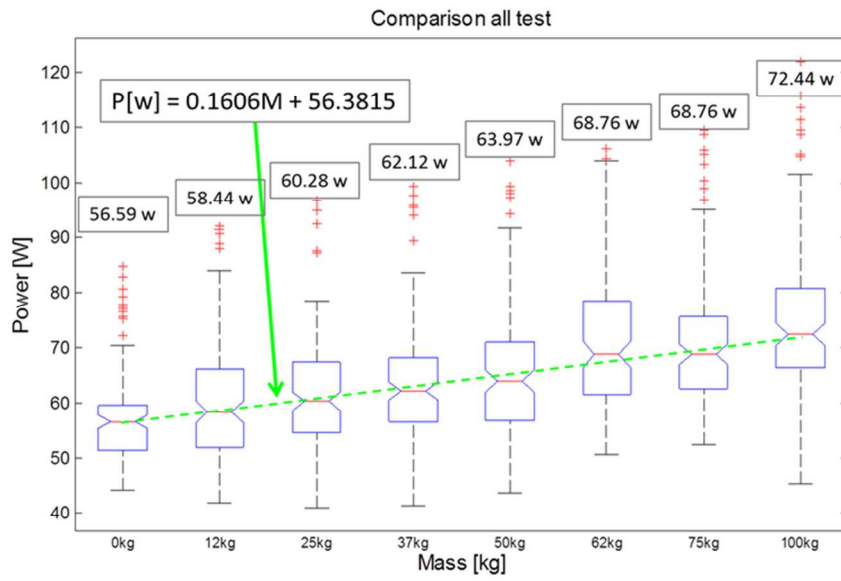


Figure 10. Results of the energy consumption of the robot gait with several loads on it.

150x94mm (150 x 150 DPI)

Industrial Robot

1
2
3
4
5
6
7
8
9
10
11
12
13
14
15
16
17
18
19
20
21
22
23
24
25
26
27
28
29
30
31
32
33
34
35
36
37
38
39
40
41
42
43
44
45
46
47
48
49
50
51
52
53
54
55
56
57
58
59
60